EARTH SURFACE PROCESSES AND LANDFORMS
Earth Surf. Process. Landforms (2017)

Published online in Wiley Online Library
(wileyonlinelibrary.com) DOI: 10.1002/esp.4143

Geomorphic process from topographic form: automating the interpretation of repeat survey data in river valleys

Alan Kasprak,[1]* Joshua Caster,[1] Sara G. Bangen[2] and Joel B. Sankey[1]
[1] Grand Canyon Monitoring and Research Center, Southwest Biological Science Center, US Geological Survey, Flagstaff, AZ USA
[2] Department of Watershed Sciences, Utah State University, Logan, UT USA

Received 10 November 2016; Revised 2 March 2017; Accepted 8 March 2017

*Correspondence to: Alan Kasprak, Grand Canyon Monitoring and Research Center, Southwest Biological Science Center, US Geological Survey, Flagstaff, AZ 86001, USA. E-mail: akasprak@usgs.gov

ESPL
Earth Surface Processes and Landforms

ABSTRACT: The ability to quantify the processes driving geomorphic change in river valley margins is vital to geomorphologists seeking to understand the relative role of transport mechanisms (e.g. fluvial, aeolian, and hillslope processes) in landscape dynamics. High-resolution, repeat topographic data are becoming readily available to geomorphologists. By contrasting digital elevation models derived from repeat surveys, the transport processes driving topographic changes can be inferred, a method termed 'mechanistic segregation.' Unfortunately, mechanistic segregation largely relies on subjective and time consuming manual classification, which has implications both for its reproducibility and the practical scale of its application. Here we present a novel computational workflow for the mechanistic segregation of geomorphic transport processes in geospatial datasets. We apply the workflow to seven sites along the Colorado River in the Grand Canyon, where geomorphic transport is driven by a diverse suite of mechanisms. The workflow performs well when compared to field observations, with an overall predictive accuracy of 84% across 113 validation points. The approach most accurately predicts changes due to fluvial processes (100% accuracy) and aeolian processes (96%), with reduced accuracy in predictions of alluvial and colluvial processes (64% and 73%, respectively). Our workflow is designed to be applicable to a diversity of river systems and will likely provide a rapid and objective understanding of the processes driving geomorphic change at the reach and network scales. We anticipate that such an understanding will allow insight into the response of geomorphic transport processes to external forcings, such as shifts in climate, land use, or river regulation, with implications for process-based river management and restoration. Copyright © 2017 John Wiley & Sons, Ltd.

KEYWORDS: geomorphic change detection; mechanistic segregation; sediment transport; sediment connectivity

Introduction

High-resolution repeat topographic survey data have become ubiquitous in the earth sciences (Passalacqua *et al.*, 2015). The advent of rapid survey techniques such as LiDAR (light detection and ranging; Collins *et al.*, 2016) and structure-from-motion photogrammetry (Westoby *et al.*, 2012; Javernick *et al.*, 2014; Smith *et al.*, 2015) have occurred concomitantly with reductions in the cost and complexity of collecting survey data (see for example, Eitel *et al.*, 2013). As a result, geomorphologists are able to readily characterize landscape change by contrasting repeat topographic surveys, a process termed Geomorphic Change Detection (GCD; Wheaton *et al.*, 2013). In fact, the ease of topographic data collection, coupled with reductions in the cost of collecting those data, have resulted in data analysis (and not collection) emerging as a bottleneck in our understanding of geomorphic dynamics. Church (2010) argued that 'for the first time, geomorphologists confront problems of analysis in the face of arguably too many data, (p.271).'

GCD provides information about the extent, magnitude, and form of landscape changes occurring during an inter-survey period, providing vital insight to geomorphologists seeking to understand, for example, the overall sediment budget of an area (Grams *et al.*, 2015), or the spatial distribution of changes through time (Collins *et al.*, 2016). At the same time, the analysis of repeat topographic data alone does not attribute changes to specific geomorphic transport processes; that is, the reasons why topographic change occurred are not necessarily revealed. This process attribution, known as 'mechanistic segregation' (cf. Wheaton *et al.*, 2013) is typically completed via user-defined attribution of change areas (e.g. Collins *et al.*, 2016), a process that is both time consuming and subjective.

The signatures of geomorphic change underlying river and floodplain morphodynamics have received particular attention over the last several decades, progressing from observational studies to quantitative geomorphic mapping and spatial analysis (Leopold and Wolman, 1957; Baker, 1977; Ashmore, 1991; Wheaton *et al.*, 2010a; Buraas *et al.*,

2014). In river valleys, the erosion, transport, and deposition of sediment occurs through several transport mechanisms, including fluvial (by rivers), aeolian (by wind), and hillslope (by gravity and/or excess rainfall and runoff) processes. The relative contribution of each transport pathway to the total valley-scale sediment flux varies between river systems (Trimble, 1983; Belmont *et al.*, 2011; Kasprak *et al.*, 2013), and may shift in response to altered water or sediment regimes driven by changes in climate or land use (Draut, 2012; Sankey and Draut, 2014). GCD and mechanistic segregation of transport processes in digital elevation models (DEMs) and associated DEMs-of-Difference (DoDs) provide a means to quantify the relative contribution of transport processes and their variability in space and time (Wheaton *et al.*, 2013; Collins *et al.*, 2016).

Here we present a novel rapid workflow for the automated mechanistic segregation of geomorphic processes from repeat topographic survey data. We apply this workflow to seven sites where a diverse suite of sediment transport processes interact along the Colorado River in the Grand Canyon, Arizona, USA using original software available as a Python script (see https://dx.doi.org/10.5066/F73776X6) to automatically infer geomorphic processes driving change observed between topographic surveys over the 11-year period from 2002 to 2013. We subsequently validate these process interpretations through independent observations of geomorphic change made in the field. We anticipate that geomorphologists will use, evaluate, and improve this methodology and software in other river valleys worldwide.

Study Area

This study focuses on seven discrete sites spanning 320 km of the Colorado River downstream from Glen Canyon Dam, herein referred to as Grand Canyon though technically inclusive of both Marble and Grand Canyons (Figure 1A). These sites have been studied over the past ~10 years as part of the Glen Canyon Dam Adaptive Management Program, which seeks to document the effects of river regulation on the physical and biological components of Grand Canyon, and thus these sites have a rich history and availability of topographic and land cover data. In Grand Canyon and many other canyon-bound river valleys of the world, floods deposit sediment (primarily sand; Topping *et al.*, 2000) in sandbars in the lee of tributary debris fans (Schmidt, 1990; Schmidt and Rubin, 1995). A portion of this flood sediment is returned to the main channel by fluvial bar erosion, sheetwash, and gullying (Sankey and Draut, 2014; Collins *et al.*, 2016; East *et al.*, 2016). Aeolian reworking of bars also transfers fine sediment to upland dunes and hillslopes (Figure 1B; Draut, 2012; East *et al.*, 2016), defined here as surfaces within the valley bottom that are above the stage of regularly-occurring floods (approximately 1270 m^3/s; Grams *et al.*, 2015). Export of sand from upland sites occurs via aeolian transport, sheetwash, and gullying (Sankey and Draut, 2014; Collins *et al.*, 2016).

Although fine sediment is vital to recreation, ecologic health, and preservation of cultural resources along the Colorado River

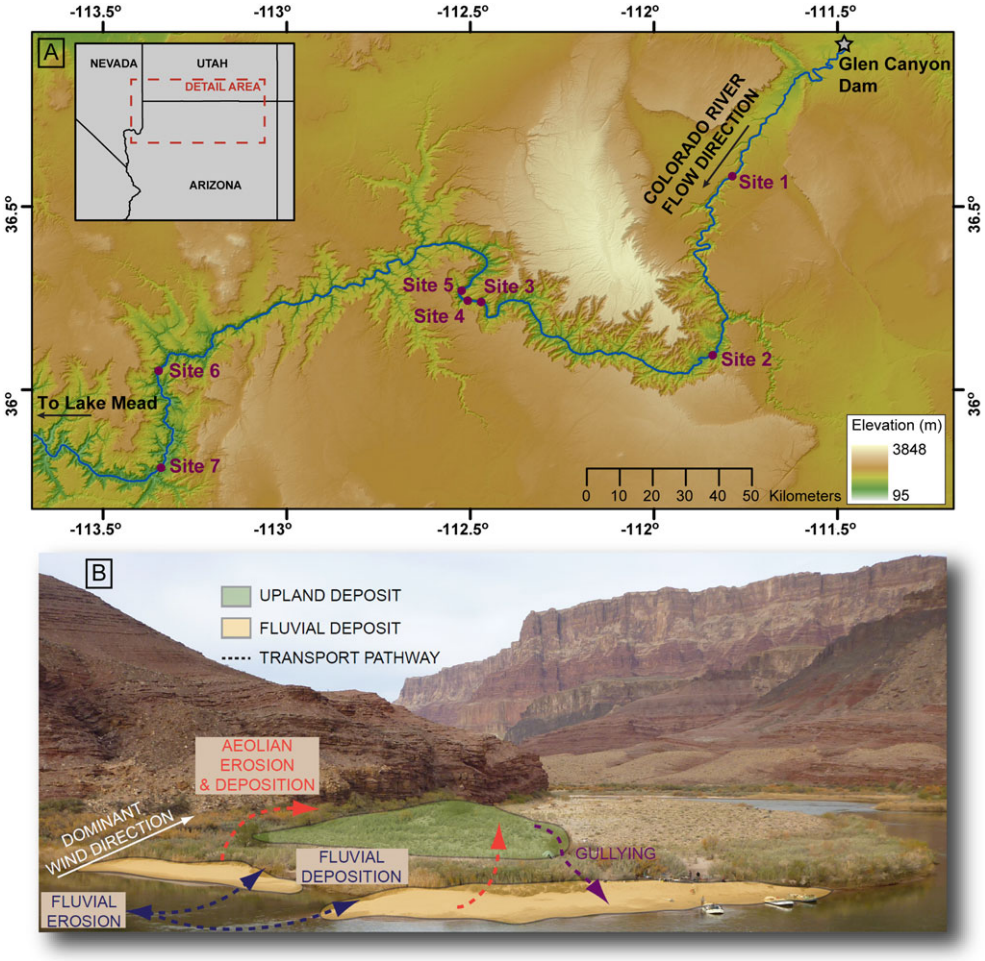

Figure 1. (A) Hillshaded digital elevation model of study area, Colorado River in the Grand Canyon, USA. Seven field validation sites used to assess predictive accuracy of geomorphic processes shown in purple. (B) Mechanisms of sediment connectivity at a coupled sandbar/upland site in the Grand Canyon; river flow direction is from left to right. [Colour figure can be viewed at wileyonlinelibrary.com]

(Schmidt *et al.*, 2001), it is also scarce. The closure of Glen Canyon Dam in 1963 (Figure 1) reduced fine sediment supply to the Grand Canyon by more than 90% (Topping *et al.*, 2000) compared to pre-dam levels. Owing to the loss of sediment supply, river managers are today faced with the challenge of quantifying the relative role of individual sediment transport processes in driving geomorphic change along a remote, extensive, and iconic river (Grams *et al.*, 2013). We note that the challenge of quantifying the relative contribution of varying sediment transport mechanisms is not unique to geomorphologists in the Grand Canyon, but rather represents a knowledge gap faced by scientists in river valleys worldwide (Belnap *et al.*, 2011).

Methods

The automated mechanistic segregation routine described here first leverages topographic data in the form of repeat digital surface models (DSMs) at 1 m resolution to produce a morphometrically-derived prediction of the mechanisms of geomorphic change at a particular site. This method is then complemented by a second set of mechanistic segregation predictions, derived from DoDs computed using the DSMs. These two approaches can be used independently of one another, or can be combined to yield a single set of predictions. Finally, we conduct field-based interpretation of the mechanisms of change at each site to validate our workflow's predictive accuracy.

DSM and DoD generation

The repeat topographic datasets used here are DSMs derived using automated photogrammetry from photographs captured via aerial overflights during May 2002, 2009, and 2013. During overflights, discharge from Glen Canyon dam was held steady at 226 m^3/s, and all subsequent analyses presented here apply to stages above this constant discharge. DSMs were generated at 1 m resolution from 0.2 m native resolution multiband aerial photographs using the Pixel Factory software suite, and are unique from traditional DEMs in that DSMs are not processed to remove vegetation. An analysis of inter-survey accuracy conducted at the locations of 187 groundtruthing panels that were deployed during the 2002 overflight revealed that the three DSM datasets had an inter-survey accuracy of 0.23 m in areas which were relatively flat (slope $< 8°$) and smooth (roughness < 2, calculated over a 3×3-cell moving window). To compute geomorphic change during the inter-survey period, we used the GCD 6 software (http://gcd.joewheaton.org; see Wheaton *et al.*, 2010b). We further assessed elevation uncertainty in the DSMs by comparing field-surveyed control point elevations with corresponding elevations derived from the DSM datasets and found that uncertainty was spatially variable and significantly influenced by both surface slope and roughness, and thus employed a fuzzy inference system (FIS; see Supporting Information) to estimate DSM uncertainty on a pixel-by-pixel basis (Bangen *et al.*, 2016).

Two DoDs were produced from the DSM datasets by differencing the 2013 and 2009 DSMs and 2009 and 2002 DSMs, respectively. On a pixel-by-pixel basis, DSM uncertainty, a function of surface slope and roughness as described earlier, was propagated as the sum of squares in quadrature (*sensu* Lane *et al.*, 2003), and subsequently compared to the magnitude of change in each pixel via a *t*-test to estimate the confidence (as a percent) that computed changes were real and not an artifact of DSM uncertainty (see Kasprak *et al.*, 2015). Areas where geomorphic change exceeded the 95% confidence threshold were retained in the final DoD.

Mechanistic segregation

Two distinct methods were used for geomorphic process attribution: (a) a landscape-based approach (LBA) for mechanistic segregation of DSMs, and (b) a DoD-based approach (DBA) for mechanistic segregation of DoDs produced from repeat topographic datasets.

Landscape-based approach (LBA)

The LBA was used to classify an area of interest (AOI) into one or more of four mechanisms of geomorphic change (Figures 2 and 3) using landscape morphometry derived from repeat topographic datasets. These mechanisms are termed *alluvial* (water-driven changes resulting from hillslope processes outside of the mainstem river channel; primarily sheetwash, rilling and gully erosion driven by excess rainfall runoff), *fluvial* (changes driven by the mainstem river channel), *aeolian*, and

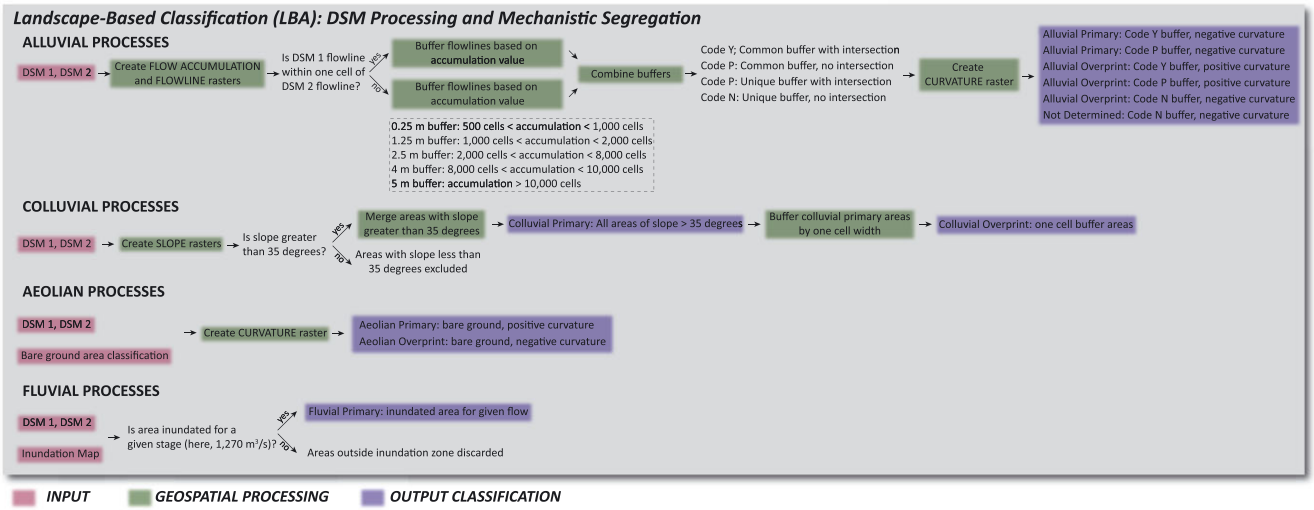

Figure 2. Generalized workflow for the landscape-based approach (LBA) used to perform mechanistic segregation of geomorphic processes at field validation sites. [Colour figure can be viewed at wileyonlinelibrary.com]

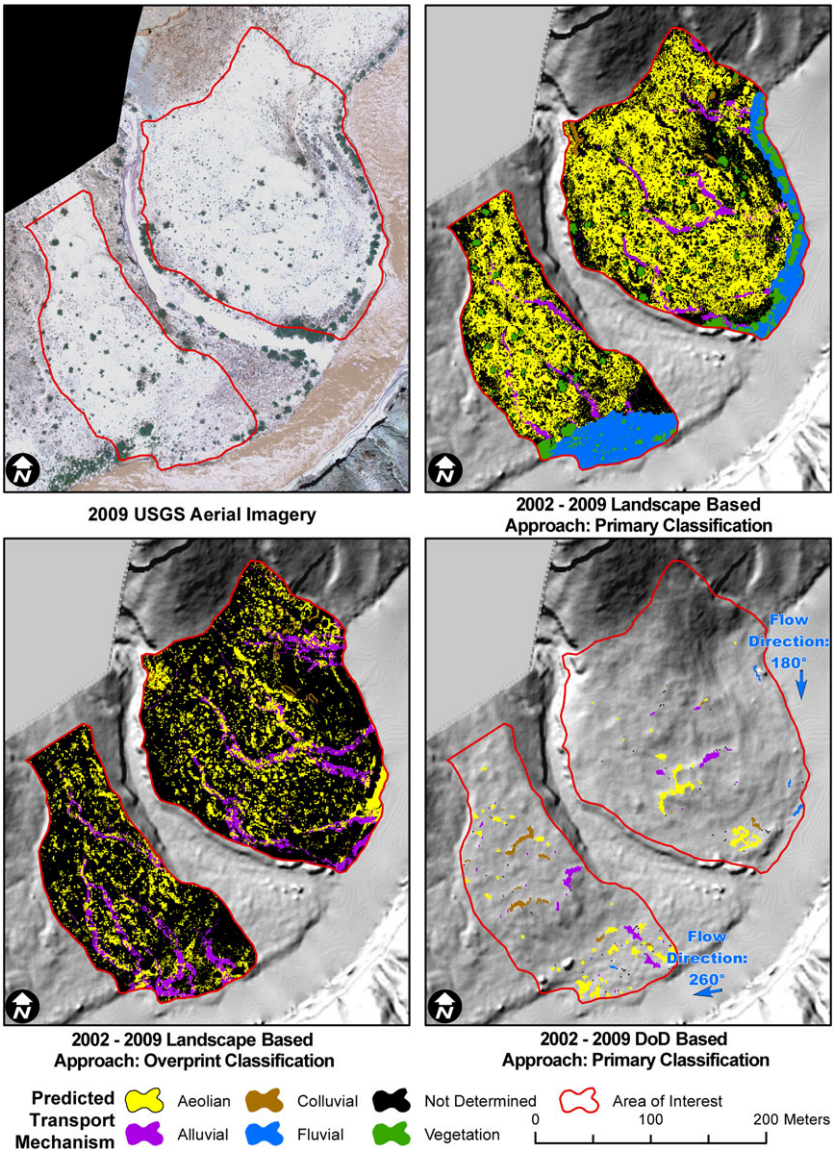

Figure 3. Landscape-based approach (LBA) and DoD-based approach (DBA) analysis for Site 1 in the Grand Canyon from 2002 to 2009. Top left panel shows 0.2 m resolution aerial photograph collected in 2009, top right panel shows primary mechanisms predicted using LBA, bottom left panel shows overprint mechanisms predicted by LBA, and bottom right panel shows mechanisms predicted by DBA. [Colour figure can be viewed at wileyonlinelibrary.com]

colluvial (gravity-driven changes expressed as mass failure). Together, these four mechanisms of change are herein referred to as 'geomorphic transport processes.' Where landscape characteristics did not result in an area being classified into one of these four mechanisms, those areas were classified as not determined. Finally, we used vegetation maps derived via semi-automated classification of aerial imagery acquired concurrently with, and registered to, the DSMs (Sankey *et al.*, 2015). Mapped vegetated areas were classified as such in the corresponding DSM data. This classification resulted in a total of six possible outcomes: alluvial, colluvial, aeolian, fluvial, not determined, or vegetated.

Where predicted, the relative role of each geomorphic transport process (fluvial, alluvial, aeolian, colluvial) was classified as either primary (i.e. the predicted process was interpreted to be the dominant driver of geomorphic change at that location), or as an overprint process (i.e. the predicted process may occur at a given location, but was likely of secondary geomorphic influence as compared to another process). Overprint processes were included here given the large temporal gaps between the DSM data collection dates (i.e. seven and four years, respectively), and it is likely that geomorphic changes at a particular location may result from a combination of transport processes; thus, the inclusion of overprinting processes allowed us to take a more inclusive approach to predicting the mechanism(s) of change for a given area. Where multiple geomorphic transport processes were initially predicted with primary or overprint status for a single location, a simple ruleset was used to resolve conflicts and determine a single primary and overprint process (see Figure 2 and section entitled 'Transport mechanism conflict resolution').

To produce a mechanistic segregation, six input datasets are required for the LBA (Figure 2). These include (a) two repeat raster topographic datasets, (b) a polygon vector mask representing the AOI for classification, here drawn to include the historic topographic survey extent at each of the study sites, while excluding any large tributary channels and their canyons, (c) a polygon vector dataset denoting vegetation coverage in the AOI (described earlier), (d) a polygon vector dataset depicting bare sediment in the AOI, and (e) vector polygons denoting the wetted and dry areas for a flood stage of interest. The inundation vectors were obtained from the step-backwater flow model produced by Magirl *et al.* (2008), and were used in

the LBA to estimate areas prone to fluvial changes. Here we used the extent of regularly-occurring postdam floods in the Grand Canyon, 1270 m^3/s (Grams *et al.*, 2015).

From the input datasets, the LBA entails the generation of three intermediary spatial datasets: a flow accumulation model, a slope model, and a curvature model (Greenlee, 1987; Jenson and Domingue, 1988; Tarboton *et al.*, 1991) which were used in combination with the input datasets to derive a mechanistic segregation for the entire AOI. Flow accumulation was calculated from both input DSMs using the ArcHydro toolbox within ArcMap 10.3. Flow accumulation values were classified into five bins based on empirical relationships between calculated flow accumulation values and measured drainage widths. These five groups were then converted to vector flowlines. The curvature model was calculated from both input DSMs, again using the curvature tool in ArcMap 10.3 which computes both slope-parallel (e.g. profile) and slope-normal (e.g. planform) curvature using a 3×3-cell moving window and combines these two datasets to yield an output curvature raster. The output of the curvature was smoothed using focal statistics with a $3\,m \times 3\,m$ moving window to calculate the mean curvature across the raster domain, which was then binned into three groups: concave (curvature < -2.5), convex (small negative and positive values from -2.5 to 5), and sharply convex (curvature > 5). Slope was computed from both input DSMs using the slope tool in the Spatial Analyst Toolbox in ArcMap 10.3. The output was binned into two groups, termed 'steep' and 'shallow', with the threshold between these set at 35°, the average frictional angle for sandy, unconsolidated substrate (U.S. Bureau of Reclamation, 1998).

LBA mechanistic segregation and process interaction

The input data and intermediary products described earlier were used to segregate the entire AOI into discrete regions based on the primary mechanism of geomorphic change predicted there. Following this initial mechanistic segregation, the likelihood for secondary, or 'overprint' geomorphic transport mechanisms to occur across the AOI was also assessed. These steps are described in detail in the sections that follow and shown in Figure 2.

Alluvial mechanism. To classify areas where geomorphic change driven by alluvial transport was likely, flow lines derived from both input DEMs were compared to assess their spatial coherence, or overlap (Figure 2). Where flow lines were within one raster cell's distance of each other, they were designated as 'common flow lines'. Where flow lines were separated by more than one raster cell's distance (e.g. 1 m), they were designated as 'unique flow lines'. We estimated the channel width associated with each flowline group using field-based observations of the relationship between flow accumulation area and the width of small drainages collected during Grand Canyon river trips. Using this relationship, we computed buffers for each flow line. These buffers were intersected in ArcMap 10.3 and coded into three groups (Figure 2): 'code Y' denoted the intersection of common flow line buffers, 'code P' denoted the intersection of unique flow line buffers or common flow line buffers without intersection, and 'code N' denoted unique flow line buffers without intersection. The grouped flow line buffers were then intersected with the concave curvature raster described earlier and subdivided into three additional groups (Figure 2): 'alluvial primary' denoted code Y and code P flow line buffers with a concave curvature, 'alluvial overprint' denoted code Y or P with a convex curvature or code N with a concave curvature, and 'not determined primary/overprint' denoted code N with a convex curvature.

Colluvial mechanism. To classify areas prone to geomorphic change driven by colluvial processes, the steep slope classification (i.e. slopes exceeding 35°; see earlier) created from both DEMs were merged into a single layer, and all areas of this layer were classified as 'colluvial primary'. A buffer of one raster cell value around the group was added and classified as 'colluvial overprint' to account for material sourced from these areas of steep slope that may have been deposited on adjacent surfaces.

Aeolian mechanism. To classify areas susceptible to aeolian change, all areas of non-vegetated sand were intersected with the convex curvature layer calculated using both input DEMs and classified into two groups. Areas of bare sand with convex curvature were classified as 'aeolian primary', and areas of bare sand that did not have a convex curvature were classified as 'aeolian overprint'.

Fluvial mechanism. To classify areas prone to fluvial geomorphic change, the AOI was split into two regions based on elevation relative to the stage of the regularly-occurring controlled flood discharge of 1270 m^3/s, presumed to be the upper limit of fluvial transport occurring in Grand Canyon. All areas below this stage were classified as 'fluvial primary', and all areas above this stage were classified as 'not determined primary'.

Transport mechanism conflict resolution. The LBA completes mechanistic segregation separately for each geomorphic transport process described earlier in three stages: (1) intersection of the alluvial, colluvial and aeolian mechanistic segregation products, (2) intersection of the product of stage one with the fluvial mechanism prediction, and (3) intersection of the product of stage two with a layer depicting the areal extent of vegetation within the AOI. As a result, the initial output may predict multiple processes for the same area (e.g. multiple primary or overprint processes). These intersections can result in three outcomes for any given area within the AOI: (1) a single primary and/or a single overprint mechanism is coded, (2) more than one primary mechanism is coded, and (3) more than one overprint mechanism is coded. To resolve conflicts in mechanistic segregation occurring in cases (2) and (3), a simple ruleset was developed to resolve conflicts and produce a maximum of one primary and overprint mechanism prediction for each pixel of the AOI, presented in Table I, which clarifies the final primary and overprint mechanisms retained when conflicts arose during classification. For any areas of the AOI not classified into one of five mechanisms (alluvial, colluvial, aeolian, fluvial, vegetation), the primary and overprint mechanisms were classified as 'not determined'. At the completion of this step, all areas within the AOI were assigned both a primary and overprint mechanism or classified as 'not determined'.

DoD-based approach (DBA)

The second method for geomorphic process attribution, the DBA, classified changes observed in a DoD into one of the four aforementioned transport processes (fluvial, alluvial, colluvial, and aeolian). The method is outlined in Figure 4 and Table II and example results are shown in Figure 3. The DBA required three inputs: (a) a raster DoD derived from repeat topographic data, (b) vectors denoting the wetted and dry areas for a flood stage of interest, which were identical to those described previously in the section entitled "Landscape-based approach", and (c) the azimuth angle of the adjacent reach of the mainstem river channel. For the DBA, we used the 1 m resolution DoD described earlier, inundation extent polygons (e.g. vectors) described earlier, and river channel azimuth angles mapped in 2013 aerial photography for the seven sites analyzed here.

Table I. Geomorphic attribution rule set for mechanism interaction processing stages

Mechanism 1	Mechanism 2	Mechanism retained	Additional change
Scenario 1: single mechanism			
Colluvial	NA/not determined	Colluvial	NA
Aeolian	NA/not determined	Aeolian	NA
Alluvial: all codes	NA/not Determined	Alluvial	NA
Scenario 2: multiple primary mechanisms			
Colluvial	Alluvial: all codes	Colluvial	Overprint coded alluvial
Colluvial	Aeolian	Colluvial	Overprint coded aeolian
Aeolian	Alluvial: code Y	Alluvial	Overprint coded aeolian
Aeolian	Alluvial: code P	Aeolian	Overprint coded alluvial
Aeolian	Alluvial: code N	Aeolian	Overprint coded alluvial
Fluvial	Colluvial	Fluvial	Overprint coded colluvial
Fluvial	Alluvial: all codes	Fluvial	Overprint coded alluvial
Fluvial	Aeolian	Fluvial	Overprint coded aeolian
NA/not determined	NA/not determined	Not determined	Overprint coded not determined
Vegetation	Fluvial	Vegetation	Overprint coded not determined
Vegetation	Colluvial	Vegetation	Overprint coded not determined
Vegetation	Alluvial: all codes	Vegetation	Overprint coded not determined
Vegetation	Aeolian	Vegetation	Overprint coded not determined
Scenario 3: multiple overprint mechanisms			
Colluvial	Alluvial: all codes	Alluvial	NA
Colluvial	Aeolian	Aeolian	NA
Aeolian	Alluvial: code Y	Alluvial	NA
Aeolian	Alluvial: code P	Aeolian	NA
Aeolian	Alluvial: code N	Aeolian	NA

Note: Scenario 1 represents geomorphic intersections with a single primary and/or overprint mechanism. Scenario 2 represents geomorphic intersections with two or more primary mechanisms. Scenario 3 represents geomorphic intersections with two or more overprint mechanisms. NA/not determined represents no data or a mechanism of not determined.

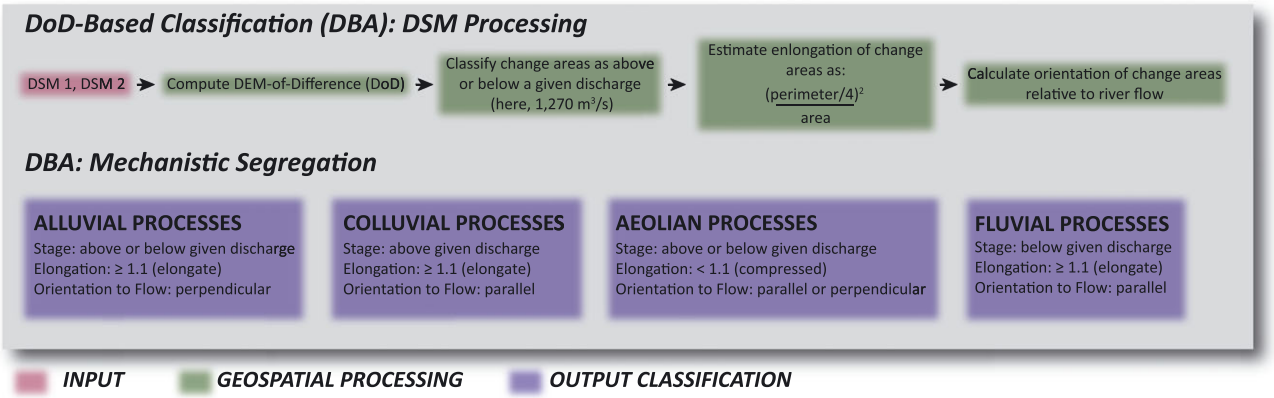

Figure 4. Generalized workflow for the DoD-based approach (DBA) used to perform mechanistic segregation of geomorphic processes at field validation sites. [Colour figure can be viewed at wileyonlinelibrary.com]

Table II. Geomorphic attribution rule set applied to apparent change based on four factors

Area	Elevation	Orientation	Elongation	Mechanism
< Raster cell value	NA	NA	NA	Insignificant
> Raster cell value	Above flood elevation	Parallel to shore line	> 1.1	Colluvial
> Raster cell value	Above flood elevation	Parallel to shore line	< 1.1	Aeolian
> Raster cell value	Above flood elevation	Perpendicular to shore line	> 1.1	Alluvial
> Raster cell value	Above flood elevation	Perpendicular to shore line	< 1.1	Aeolian
> Raster cell value	Below flood elevation	Parallel to shore line	> 1.1	Fluvial
> Raster cell value	Below flood elevation	Parallel to shore line	< 1.1	Aeolian
> Raster cell value	Below flood elevation	Perpendicular to shore line	> 1.1	Alluvial
> Raster cell value	Below flood elevation	Perpendicular to shore line	< 1.1	Aeolian

Note: For this project, flood elevation represents the maximum controlled flow stage of 1270 m^3/s. An empirical threshold of 1.1 was used to separate elongate and round (i.e. non-elongate) polygons. NA, data not available.

The input DoD dataset was transformed to a binary vector dataset where all areas of change were classified as either positive (i.e. deposition) or negative (i.e. erosion). The area for each polygon within this vector dataset was then calculated. All polygons with area less than the original raster cell resolution were designated as insignificant change and discarded. For the remaining polygons, three morphometric characteristics were calculated to infer a predicted mechanism of change: (1) polygon elevation relative to flood stage of interest, (2) polygon orientation and (3) polygon elongation factor. The elevation was determined by the percent of polygon area above and below a given flood stage, here set at the stage corresponding to the maximum regularly-occurring flood discharge of 1270 m^3/s. Those polygons with more than 50% area above this elevation were classified as 'above,' and polygons with more than 50% area at or below the typical flood elevation are classified as 'below'.

The orientation factor required two intermediate calculations: (a) minimum enclosing rectangles, using the Minimum Bounding Geometry tool in ArcMap, which was used here to compute the smallest rectangle that would enclose, or bound, any given polygon of elevation change in the DoD and (b) polygon orientations calculated from those rectangles using the Calculate Polygon Main Angle tool in ArcMap, which calculates the angle of the longest group of line segments forming a given polygon. An orientation classification of 'parallel' was assigned to polygons with orientation less than ±45° of the azimuth angle of the Colorado River shore line adjacent to each study site, whereas a classification of 'perpendicular' was made for polygons with orientation greater than ±45° with respect to the shoreline azimuth angle.

The elongation factor (F_E) was calculated using the area and perimeter of the minimum enclosing rectangle as follows:

$$F_E = \left(\frac{P}{4}\right)^2 A^{-1} \quad (1)$$

where P is the perimeter and A is the area of the polygon of interest.

These three characteristics were used to estimate a predicted geomorphic transport mechanism based on four assumptions derived from field and remote sensing observations of the study area and other river systems undergoing similar geomorphic transport processes:

- Alluvial change tends to be elongated and oriented either parallel to the dominant slope or perpendicular to the orientation of the mainstem river channel
- Aeolian change tends to occur in round patches (i.e. not elongated in any particular direction) with no preferential orientation relative to the river channel
- Fluvial change tends to occur within the typical flood stage and is elongated parallel to channel flow
- Colluvial change tends to occur perpendicular to dominant slope and parallel to the lowest dominant landform (i.e. the Colorado River). In essence, colluvial processes tend to remove material from steeply-sloping, river-oblique valley walls and deposit this material parallel to the river channel.

Field-based validation

We assessed the accuracy of automated mechanistic segregation by comparing predicted mechanisms to field observations at discrete locations (i.e. points) within the seven analysis sites in May of 2016. At each site (Figure 1), we selected between 13 and 23 validation points using 0.2 m resolution aerial imagery collected in 2013 (the most recent high-resolution image set available for Grand Canyon), for a total of 113 comparison points. The points were pre-selected for their accessibility in the field (e.g. located in areas where we anticipated the point could be safely visited on foot during field visits). Although the dates of imagery and DSM datasets preceded our field visits by several years, previous field campaigns had visited these sites for related studies and as such we were confident that no large-scale geomorphic reworking of the areas (e.g. flash floods or major slope failures) had occurred there in the time between 2013 image collection and our visits in the spring of 2016. We visited each pre-selected validation point in May of 2016. Given the limited reliability of global positioning system (GPS) at the bottom of Grand Canyon, we navigated to each point using its marked location on 0.2 m resolution photographs, and we were generally able to navigate confidently to within ~1 m of any given validation point.

To assess the accuracy of mechanistic segregation, we developed process indicators for each transport mechanism (East *et al.*, 2016; Table III). At each validation point, the likelihood of a given transport process being responsible for change was assessed as a function of these indicators and assigned into one of three categories: *likely* meant that the process was either observed in the field or geomorphic indicators provided evidence that it had or would soon occur; *plausible* meant that the morphometry of the site was such that the process could conceivably occur there, even if there was no evidence of it recently having occurred; finally, *unlikely* meant that the morphometry of the site was not conducive to the predicted process occurring there, nor was there evidence of the process having occurred. For any points classified as not determined (see earlier) that were located within 0.5 m of an area classified as one of the four geomorphic transport processes, the point was instead assessed for that process given (a) limits on our ability to navigate to any point with an accuracy <1 m, and (b) the fact that we were better able to observe the occurrence of transport processes than a lack thereof in the field.

Results

At the 113 validation points for the two periods 2002–2009 and 2009–2013, the LBA produced 452 individual predictions of geomorphic processes (226 primary, 226 overprint). For brevity, here we report mainly on the 226 primary mechanism predictions made using the LBA. The DBA returned 50 individual predictions, markedly less than the number of predictions from the LBA; this is because relatively few validation points exhibited geomorphic change in the resultant DoDs, and as such DBA predictions were not made for all validation points. This is in contrast to the LBA, which makes predictions of the transport mechanism that would occur at a given location, regardless of whether appreciable geomorphic change actually occurred there during the inter-survey period. Across the LBA validation points, predicted geomorphic transport processes generally agreed with field-observed mechanisms of change: 88% of LBA-generated predictions were classified as either likely or plausible in the field (Figure 5). The DBA also produced generally accurate predictions: 72% of its predictions were classified as likely or plausible during field visits (Figure 5).

Prediction accuracy varied by the mechanism being examined. For validation points where fluvial processes were predicted by either the LBA or DBA, 100% of field observations indicated evidence of fluvial processes (for indicators, see Table III). In the case of aeolian predictions, field observations were in agreement with predictions 96% of the time. Colluvial

Table III. Indicators of geomorphic transport processes used to assess landscape-based approach (LBA) and DoD-based approach (DBA) predictions at validation points in Grand Canyon

Mechanism	'Likely' indicators:	'Plausible' indicators:
Aeolian transport *Wind-driven transport at any stage*	• Observed aeolian erosion/deposition • Wind ripples • Sand shadows • Dunes or dune blow-out morphology • Aeolian sediment lining gullies • Eroded or buried vegetation outside of topographic depressions	• Areas of bare sand above the stage of contemporary maximum floods (1270 m^3/s shoreline in the Grand Canyon) • Burial of biological soil crust
Alluvial transport *Water-driven transport above 1270 m^3/s stage*	• Observed alluvial transport • Eroded/buried vegetation in gullies • Fresh sediment deposits in arroyos, gullies or rills • Evidence of instability within arroyos, gullies, or rills (e.g. bank undercutting/slumping, knick points, or abrupt changes in channel characteristics) • Sediment containing material coarser than sand (i.e. not the result of aeolian transport)	• Presence of arroyos, gullies, or rills • Topographic flowpaths without active channels
Fluvial transport *Water-driven transport below 1270 m^3/s stage*	• Observed fluvial erosion or deposition • Deposits with flood stratigraphy • Bench formation on beaches • Deposition of wood or other debris • Swash marks on beach	• Areas of bare sand below the stage of contemporary maximum floods (1270 m^3/s shoreline in Grand Canyon) • Areas known to have undergone change during floods from aerial photographs
Colluvial transport *Gravity-driven transport at any stage*	• Observed mass wasting • Slump blocks below slope • Sediment at/near angle of repose • Burial of plants near base of slope • Exposure of roots along slope • Surface cracking on slope	• Surfaces at or near angle of repose

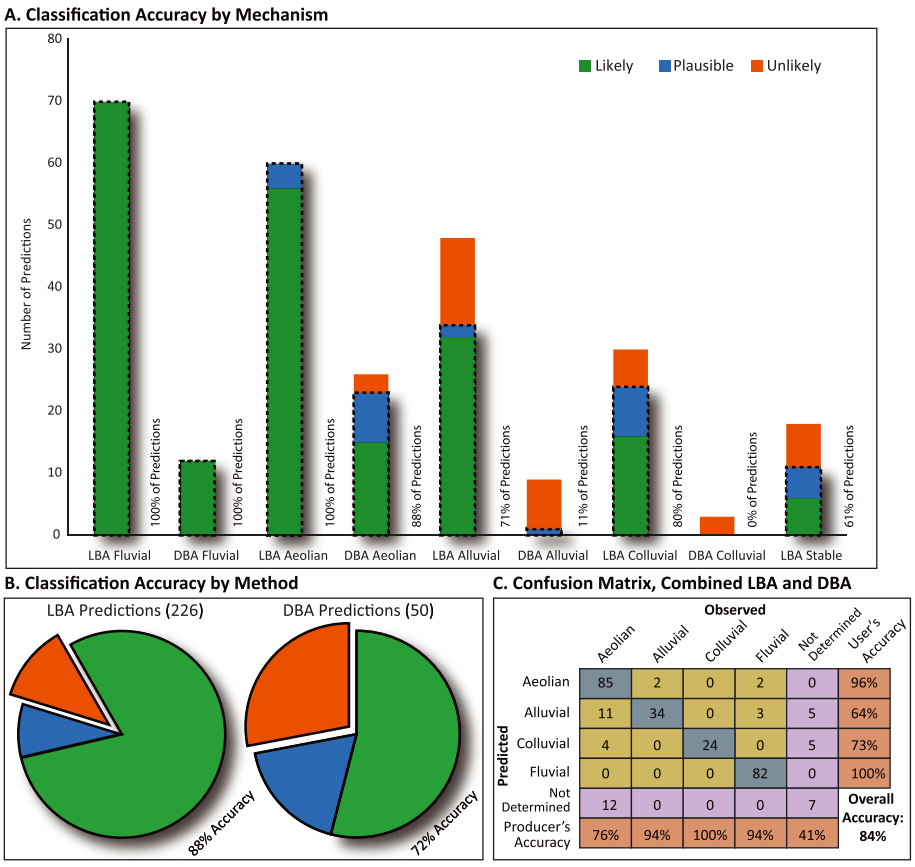

Figure 5. Assessment of landscape-based approach (LBA) and DoD-based approach (DBA) classification accuracy for time periods 2002–2009 and 2009–2013. (A) Shows predictive accuracy of LBA and DBA methods by mechanism assessed, (B) depicts individual classification accuracy of LBA and DBA methods, and (C) shows confusion matrix of all validation points for LBA and DBA methods. [Colour figure can be viewed at wileyonlinelibrary.com]

and alluvial predictions were confirmed by field observations in 73% and 64% of instances, respectively (Figure 5). The factors leading to classification error varied depending on the classification approach being used. In the case of the LBA, the most frequent instances of classification error were found when geomorphic change was predicted at a validation point, but that point was observed to be stable in the field, with no indication of recent sediment transport (six instances out of 226 total LBA mechanism predictions). For the DBA, mis-classification could most often be attributed to instances of alluvial predictions which were instead found to be the result of aeolian processes when field-checked (four instances out of nine total DBA alluvial predictions); these were all aeolian interdune areas elongated perpendicular to the mainstem river flow.

The degree to which the LBA and DBA agree may provide an estimate of confidence in their predictions. In the 29 instances that the LBA's primary mechanism agreed with the DBA primary mechanism, field observations confirmed this prediction as correct 97% of the time. When the LBA's primary mechanism and the DBA's predicted mechanism disagreed (21 instances), the LBA primary mechanism agreed with field observations more often (91% of instances likely or plausible) than did the DBA prediction (33%). Finally, although the majority of our analysis focused on an assessment of the LBA primary and DBA predictions, we performed an assessment of the LBA overprint predictions at the 50 sites where both the LBA and DBA produced predictions. There, for the 12 sites where the LBA primary mechanism was classified as plausible or unlikely (i.e. we had reduced confidence in its predictive accuracy), the LBA overprint mechanism was classified as likely 67% of the time, which may suggest its utility as a secondary prediction in areas where the primary mechanism is unlikely to occur.

Discussion

The widespread use of airborne and ground-based high-resolution sampling techniques such as automated photogrammetry, structure-from-motion, LiDAR, real-time kinematic (RTK)-GPS, or total station and stadia rod (see, for example, www.opentopography.org and www.ned.usgs.gov; also see Wheaton *et al.*, 2010b; Smith *et al.*, 2015) means that geomorphologists are readily able to collect repeat topographic data at a pace that far outstrips their ability to quantitatively analyze landscape change (Church, 2010). The automated methods presented here provide a way forward in the rapid mechanistic segregation of geomorphic change in DEMs and DoDs. Overall, both the LBA and DBA methods performed well when compared to field observations of geomorphic transport processes at seven sites along the Colorado River in Grand Canyon (Figures 1 and 5), with the LBA performing slightly better (88% of predictions were confirmed during field visits) than the DBA (72% of predictions confirmed).

Predictive errors in classification of geomorphic transport mechanisms could be the result of three scenarios: (1) cases in which a predicted mechanism was classified as unlikely in the field, but where another mechanism that was also predicted was likely to be occurring (e.g. LBA primary mechanism was unlikely, but DBA mechanism was likely or plausible), (2) instances where a mechanism of change was predicted but the site was found to be stable, with no evidence of recent geomorphic change, or (3) instances where a mechanism other than those predicted by the LBA or DBA was found to be occurring. In the case of the LBA, the most frequent cause of classification error was scenario (2) (predicted change but site observed to be stable). This is unsurprising, as the LBA relies on landscape morphometry to derive likely mechanisms of geomorphic change, and does not take into account whether areas exhibited appreciable geomorphic change over time (Figure 2). In the case of the DBA, the most frequent cause of mis-classification error was scenario (3) (a mechanism other than that predicted was observed; 14 instances total), and this was most often due to alluvial change being observed as aeolian in the field (four instances).

The data requirements of our workflow, as they relate to its broader applicability within the geomorphic community, are worth consideration. The LBA requires repeat topographic surveys (Figure 2); here we employed 1 m DSM datasets at temporal intervals of seven and four years, but no user constraints are placed on the collection interval of topographic data. In addition, the LBA requires vector datasets of vegetation and bare sediment extent, the former to exclude vegetated areas from mechanistic segregation and the latter to delineate areas with the potential to undergo aeolian transport. While we used vegetation and bare sand coverages derived from semi-automated remote sensing image analysis and classification methods (Maurer and Gerke, 2011; Sankey *et al.*, 2015), mapping from field visits and/or aerial photograph or LiDAR point cloud analysis and subsequent polygon digitization may prove equally acceptable. Finally, the LBA requires an estimate of the extent of fluvial processes via inundation polygons (typically derived from a one-dimensional flow model or field mapping of high water indicators; Costa and O'Connor, 1995; Horritt and Bates, 2002) that reflect the geomorphically-effective flow in the study area. The choice of flow will vary by site. Here we used the inundation extent of regularly-occurring high flow dam releases (Schmidt *et al.*, 2001; Grams *et al.*, 2015) of 1270 m^3/s, the contemporary maximum flood stage in Grand Canyon. In many river valleys, we surmise that the area susceptible to fluvial processes may correspond to the inundation extent of regularly-occurring floods (e.g. $Q_{1.5}$, Q_2, or the bankfull flow; Leopold *et al.*, 1965). However, in landscapes influenced by recent episodic floods that may be responsible for a great deal of geomorphic work across large extents of the river valley (e.g. Gartner *et al.*, 2015; Dethier *et al.*, 2016), inundation polygons corresponding to more extreme flows may be justified. We acknowledge that the workflow's development and implementation was made possible in large part due to the wealth of auxiliary hydrologic and land cover data already available in Grand Canyon (e.g. stage and vegetation/sand mapping) from previous research there. At the same time, we believe that the added time and effort required for production of these datasets in other river corridors will likely prove worthwhile for the implementation of our workflow there, particularly when mechanistic segregation over large spatial areas and/or in a *post hoc* manner for large volumes of historic topographic data are desired.

The DBA presented here requires a raster DoD of geomorphic change; we used a DoD depicting changes at a 95% confidence interval (see earlier), though in practice the choice of DEM survey interval and DoD thresholding is left to the user. While conservative, we found that the 95% confidence interval most accurately reflected areas of change observed in the field while excluding spurious changes arising from survey noise (Kasprak *et al.*, 2015). In addition, the DBA requires the aforementioned inundation polygons that correspond to the zone of fluvial processes at the study site. Finally, though we have attempted to achieve scale-independence in the workflow (e.g. using cell widths in lieu of distance units for buffers whenever possible; Figure 4), the choice of buffer width for drainage delineation in the alluvial

component of the LBA requires users to estimate the influence width of drainage pathways based on their upstream accumulation area. In this case, we used empirical data and field observations from Grand Canyon to derive these relationships (Sankey and Draut, 2014), and suggest that a similar approach is justified when extending the workflow to additional sites.

We suspect that the two approaches here may be best suited for topographic data of varying resolutions (Figure 6, Table IV). In the case of the LBA, patterns in landscape morphometry at the scale of 10^0 to $10^2\,m^2$ may provide insight into the geomorphic transport processes likely to be occurring there. DSMs and DEMs that provide information at these scales (e.g. pixel resolutions of 1 to 10 m) may be ideal for the rapid delineation of landscape areas susceptible to varying mechanisms of geomorphic change (e.g. alluvial, colluvial, fluvial, aeolian). The high degree of accuracy with which the LBA was able to predict the dominant mechanism(s) of geomorphic change when compared to field observations (88%) using 1 m DSM data indicates that the method is well suited to these relatively coarse resolution data collected over broad landscape areas. However, our observation that the DBA exhibited less overall accuracy of predictions (72%) than the LBA may suggest that the requisite computation of morphodynamic signatures (e.g. concavity, elongation, orientation to river flow) in DoDs may benefit from higher-resolution data with smaller pixel sizes. In particular, the accurate delineation of changes due to alluvial processes in the DBA requires continuously capturing geomorphic change along drainage pathways; with coarser data or more conservative DoD thresholding, areas of change as seen in a raster DoD may become discontinuous and patchy. Similarly, a DBA classification of aeolian change implies discrete areas with no preferential orientation; with coarser DoD resolution, these areas may become merged along the dominant wind direction. Both of these instances are illustrated in Figure 6, which was produced by implementing both the LBA and DBA on DEMs collected using a terrestrial laser scanner at Site 5 and incrementally downsampling the datasets from the original resolution of 0.05 m to 0.25 m, 0.5 m, and 1 m resolution. In both Figure 6 and Table IV, incremental loss of resolution appears to significantly alter the results of DBA classification, particularly with regard to alluvial and aeolian predictions, which progressively decrease in overall contribution to predicted geomorphic change as DEM resolution coarsens.

Table IV. Relative contribution (as percent of overall area of predicted change) using landscape-based approach (LBA) and DoD-based approach (DBA) to analyze digital elevation models (DEMs) of decreasing resolution at Site 5 in Grand Canyon

Mechanism	0.05 m Resolution	0.25 m Resolution	0.5 m Resolution	1.0 m Resolution
Landscape-based approach (LBA)				
Aeolian	44.30%	43.51%	37.21%	39.35%
Alluvial	0.16%	1.66%	14.56%	1.49%
Fluvial	9.97%	10.02%	8.81%	1.96%
Colluvial	13.10%	13.19%	13.24%	13.12%
Not determined	18.70%	17.85%	12.50%	30.29%
Vegetation	13.77%	13.77%	13.69%	13.78%
DoD-based approach (DBA)				
Aeolian	41.17%	35.79%	43.91%	11.09%
Alluvial	33.04%	11.70%	5.37%	8.70%
Fluvial	11.13%	13.68%	8.05%	8.70%
Colluvial	1.45%	4.40%	15.10%	26.09%
Not determined	13.21%	34.44%	27.56%	45.43%

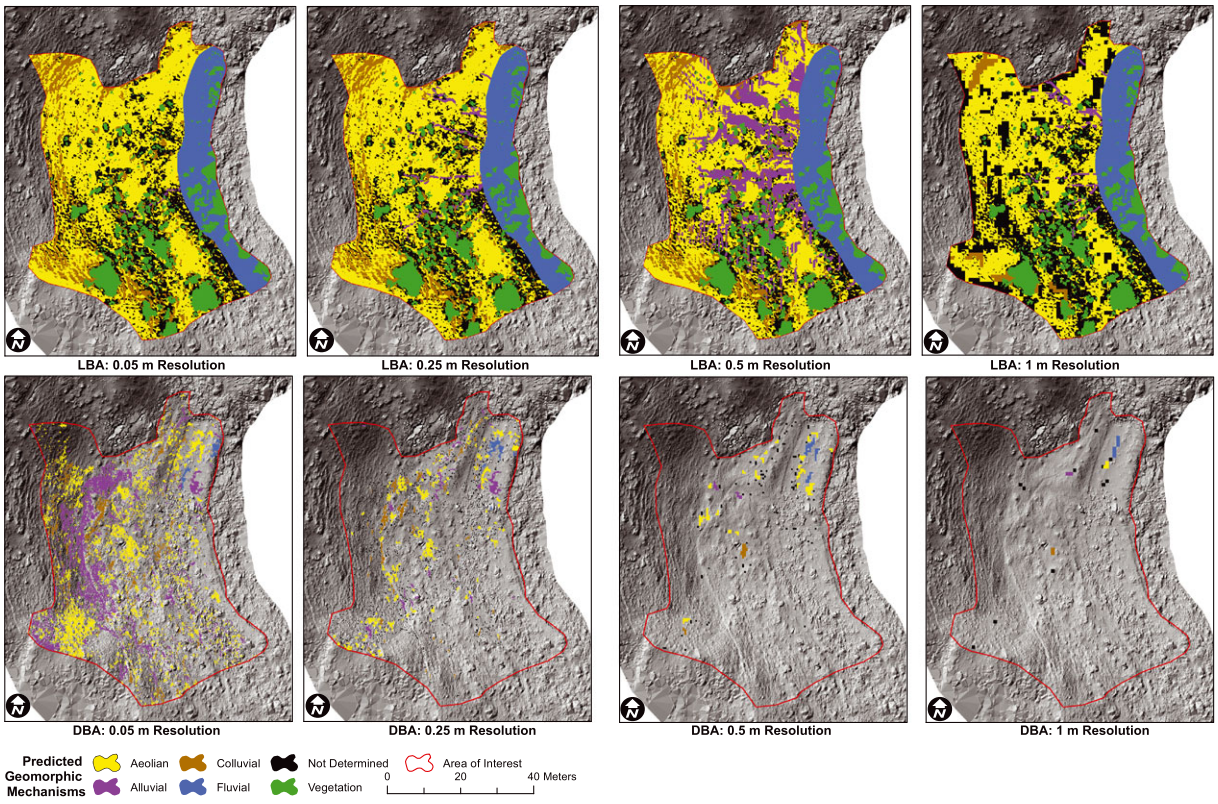

Figure 6. Effect of decreasing digital elevation model (DEM) resolution on geomorphic transport mechanism predictions of landscape-based approach (LBA) (top row) and DoD-based approach (DBA) (bottom row). The 0.05 m resolution DEM collected via terrestrial laser scanning (i.e. ground-based LiDAR) at Site 5 in Grand Canyon was downsampled to 0.25 m, 0.5 m, and 1.0 m resolutions and analyzed using LBA and DBA. [Colour figure can be viewed at wileyonlinelibrary.com]

Finally, our workflow and automated mechanistic segregation was developed for canyon-bound river valleys with the intent to make the process adaptable across a diversity of landscapes. We suspect that there are several instances where the methodology presented here may need to be augmented in order to produce accurate classification of geomorphic transport processes. For example, in silt or clay dominated river systems, increases in the angle of sediment repose due to cohesion may lead to predictive errors (i.e. overestimation of the influence of colluvial processes) in the LBA. As another example, in river valleys with large biological influences on sediment transport (for example, beaver dam construction or tree throw; Gabet *et al.*, 2003; Bouwes *et al.*, 2016), the mechanisms of geomorphic change would not be accurately predicted in our workflow without the addition of a biological component. In general, however, we believe that for the majority of river valleys – and particularly canyon-bound rivers – where repeat topographic data are available and where physical processes (and not biologic) dominate sediment transport, our methodology is likely to perform well. Finally, the workflow presented here may prove useful in the development of site-scale mechanistic sediment budgets, specifically through tracking the location of erosion/deposition locations and their driving mechanism(s) through time, resulting in a quantitative analysis of sediment routing through a given site; although these components are not currently part of the workflow, they represent a potential avenue for further study and software modification.

Conclusions

The methodology for the automated mechanistic segregation of geomorphic transport processes in repeat topographic data presented here provides a more objective and automated process for earth scientists to interpret landscape change from high-resolution survey data at or near the pace with which it is currently being collected. Further testing should focus on applications in other river valleys throughout the world, and subsequent refinement of this workflow should consider its performance using topographic data collected at varying resolutions (e.g. pixel resolutions of 10^{-2} to 10^{2} m^{2}) and over varying temporal survey intervals (e.g. months to decades). Finally, we believe that insight into the relative utility of the LBA and DBA may be gained by employing the two approaches across a variety of river systems (Brierley and Fryirs, 2005), particularly in instances where the relative contribution of fluvial, aeolian, colluvial, and alluvial transport processes are highly variable.

Acknowledgments—This research was funded by the Bureau of Reclamation's Glen Canyon Dam Adaptive Management Program, with additional funding from a National Science Foundation award to the National Center for Earth Surface Dynamics at the University of Minnesota, Minneapolis, MN. Kasprak's work at the USGS was supported under a Mendenhall Postdoctoral Fellowship. The authors acknowledge the National Park Service and Grand Canyon National Park for providing permission to conduct field research. Data and software used in this manuscript can be accessed at https://dx.doi.org/10.5066/F73776X6. The authors thank Dan Buscombe, Amy East, Helen Fairley, Paul Grams, Jen Dierker, Jack Schmidt, and Joe Wheaton for discussion that greatly improved the manuscript, along with the suggestions of Simone Bizzi and an anonymous reviewer who provided helpful recommendations. Tom Gushue, Geoff Chain, and Terry Arundel provided and archived the geospatial data for this project. Grand Canyon boatmen Dennis Harris and Kirk Burnett were instrumental in conducting field validation work.

Disclaimer

This manuscript is submitted for publication with the understanding that the US Government is authorized to reproduce and distribute reprints for Governmental purposes. Any use of trade, product, or firm names is for descriptive purposes only and does not imply endorsement by the US Government.

References

Ashmore PE. 1991. How do gravel-bed rivers braid? *Canadian Journal of Earth Sciences* **28**: 326–341 https://doi.org/1139/e91-030

Baker VR. 1977. Stream-channel responses to floods, with examples from central Texas. *Geological Society of American Bulletin* **88**: 1057–1071 https://doi.org/1130/0016-7606(1977)88<1057

Bangen S, Hensleigh J, McHugh P, Wheaton JM. 2016. Error modeling of DEMs from topographic surveys of rivers using fuzzy inference systems. *Water Resources Research* **52**: 1176–1193 https://doi.org/1002/2015WR018299

Belmont P, Gran K, Schottler S, Wilcock P, Day S, Jennings C, Lauer JW, Viparelli E, Willenbring J, Engstrom D, Parker G. 2011. Large shift in source of fine sediment in the upper Mississippi River. *Environmental Science and Technology* **45**: 8804–8810 https://doi.org/1021/es2019109

Belnap J, Munson S, Field JP. 2011. Aeolian and fluvial processes in dryland regions: the need for integrated studies. *Ecohydrology* **4**: 615–622 https://doi.org/1002/eco.258

Bouwes N, Weber N, Jordan CE, Saunders C, Tattam IA, Volk C, Wheaton JM, Pollock MM. 2016. Ecosystem experiment reveals benefits of natural and simulated beaver dams to a threatened population of steelhead (*Oncorhynchus mykiss*). *Scientific Reports* **6**: 28581 https://doi.org/1038/srep28581

Brierley G, Fryirs K. 2005. *Geomorphology and River Management*. Blackwell Publishing: Hoboken, NJ.

Buraas EM, Renshaw CE, Magilligan FJ, Dade WB. 2014. Impact of reach geometry on stream channel sensitivity to extreme floods. *Earth Surface Processes and Landforms* **39**: 1778–1789 https://doi.org/1002/esp.3562

Church M. 2010. The trajectory of geomorphology. *Progress in Physical Geography* **34**: 265–286 https://doi.org/1177/0309133310363992

Collins BD, Bedford DR, Corbett SC, Cronkite-Ratcliff C, Fairley HC. 2016. Relations between rainfall-runoff-induced erosion and aeolian deposition at archaeological sites in a semi-arid dam-controlled river corridor. *Earth Surface Processes and Landforms* **41**: 899–917 https://doi.org/1002/esp.3874

Costa JE, O'Connor JE. 1995. Geomorphically effective floods. In *Natural and Anthropogenic Influences in Fluvial Geomorphology*, Costa JE, Miller AJ, Potter KW, Wilcock PR (eds). American Geophysical Union: Washington, DC; 45–56.

Dethier E, Magilligan FJ, Renshaw CE, Nislow KH. 2016. The role of chronic and episodic disturbances on channel-hillslope coupling: the persistence and legacy of extreme floods. *Earth Surface Processes and Landforms* **41**: 1437–1447 https://doi.org/1002/esp.3958

Draut AE. 2012. Effects of river regulation on aeolian landscapes, Colorado River, southwestern USA. *Journal of Geophysical Research: Earth Surface* **117**: F02022 https://doi.org/1029/2011JF002329

East AE, Collins BD, Sankey JB, Corbett SC, Fairley HC, Caster J. 2016. *Conditions and Processes Affecting Sand Resources at Archeological Sites in the Colorado River Corridor below Glen Canyon Dam, Arizona*, USGS Professional Paper 1825. US Geological Survey: Reston, VA. https://doi.org/3133/pp1825

Eitel JUH, Vierling LA, Magney TS. 2013. A lightweight, low cost autonomously operating terrestrial laser scanner for quantifying and monitoring ecosystem structural dynamics. *Agricultural and Forest Meteorology* **180**: 86–96 https://doi.org/1016/j.agrformet.2013.05.012

Gabet EJ, Reichman OJ, Seabloom EW. 2003. The effects of bioturbation on soil processes and sediment transport. *Annual Review of Earth and Planetary Sciences* **31**: 249–273 https://doi.org/1146/annurev.earth.31.100901.141314

Gartner JD, Dade WB, Renshaw CE, Magilligan FJ, Buraas EM. 2015. Gradients in stream power influence lateral and downstream sediment flux in floods. *Geology* **43**: 983–986 https://doi.org/1130/G36969.1

Grams PE, Schmidt JC, Wright SA, Topping DJ, Melis TS, Rubin DM. 2015. Building sandbars in the Grand Canyon. *EOS, Transactions, American Geophysical Union* **96** https://doi.org/1029/2015EO030349

Grams PE, Topping DJ, Schmidt JC, Hazel JE, Kaplinski M. 2013. Linking morphodynamic response with sediment mass balance on the Colorado River in Marble Canyon: issues of scale, geomorphic setting, and sampling design. *Journal of Geophysical Research: Earth Surface* **118**: 361–381 https://doi.org/1002/jgrf.20050

Greenlee DD.1987. Raster and vector processing for scanned linework. *Photogrammetric Engineering and Remote Sensing* **53**(10): 1383–1387.

Horritt MS, Bates PD. 2002. Evaluation of 1D and 2D numerical models for predicting river flood inundation. *Journal of Hydrology* **268**: 87–99 https://doi.org/1016/S0022-1694(02)00121-X

Javernick L, Brasington J, Caruso B. 2014. Modeling the topography of shallow braided rivers using structure-from-motion photogrammetry. *Geomorphology* **213**: 166–182 https://doi.org/1016/j.geomorph.2014.01.006

Jenson SK, Domingue JO. 1988. Extracting topographic structure from digital elevation data for geographic information system analysis. *Photogrammetric Engineering and Remote Sensing* **54**(11): 1593–1600.

Kasprak A, Magilligan FJ, Nislow KH, Renshaw CE, Snyder NP, Dade WB. 2013. Differentiating the relative importance of land cover change and geomorphic processes on fine sediment sequestration in a logged watershed. *Geomorphology* **185**: 67–77 https://doi.org/1016/j.geomorph.2012.12.005

Kasprak A, Wheaton JM, Ashmore PE, Hensleigh JW, Peirce S. 2015. The relationship between particle travel distance and channel morphology: results from physical models of braided rivers. *Journal of Geophysical Research: Earth Surface* **130**: 55–74 https://doi.org/1002/2014JF003310

Lane SN, Westaway RM, Hicks DM. 2003. Estimation of erosion and deposition volumes in a large, gravel-bed, braided river using synoptic remote sensing. *Earth Surface Processes and Landforms* **28**: 249–271 https://doi.org/1002/esp.483

Leopold L, Wolman M. 1957. *River Channel Patterns: Braided, Meandering, and Straight*, USGS Professional Paper 282-B. US Geological Survey: Reston, VA.

Leopold L, Wolman MG, Miller JP. 1965. *Fluvial Processes in Geomorphology*. Dover Earth Sciences: Mineola, NY; 544.

Magirl CM, Breedlove J, Webb RB, Griffiths P. 2008. *Modeling Water-surface Elevations and Virtual Shorelines for the Colorado River in Grand Canyon, Arizona*, USGS Scientific Investigations Report 2008–5075. US Geological Survey: Reston, VA; 32.

Maurer T, Gerke HH. 2011. Modelling aeolian sediment transport during initial soil development on an artificial catchment using WEPS and aerial images. *Soil and Tillage Research* **117**: 148–162 https://doi.org/1016/j.still.2011.09.008

Passalacqua P, Belmont P, Staley D, Simley J, Arrowsmith JR, Bode C, Crosby C, DeLong S, Glenn N, Kelly S, Lague D, Sangireddy H, Schaffrath K, Tarboton D, Wasklewicz T, Wheaton J. 2015. Analyzing high resolution topography for advancing the understanding of mass and energy transfer through landscapes. *Earth-Science Reviews* **148**: 174–193 https://doi.org/1016/j.earscirev.2015.05.012

Sankey J, Draut AE. 2014. Gully annealing by aeolian sediment: field and remote-sensing investigation of aeolian–hillslope–fluvial interactions, Colorado River corridor, Arizona, USA. *Geomorphology* **220**: 68–80 https://doi.org/1016/j.geomorph.2014.05.028

Sankey J, Ralston B, Grams P, Schmidt JC, Cagney LE. 2015. Riparian vegetation, Colorado River, and climate: five decades of spatiotemporal dynamics in the Grand Canyon with river regulation. *Journal of Geophysical Research: Biogeosciences* **120**: 1532–1547 https://doi.org/1002/2015JG002991

Schmidt JC. 1990. Recirculating flow and sedimentation in the Colorado River in Grand Canyon, Arizona. *Journal of Geology* **98**: 709–724.

Schmidt JC, Parnell RA, Grams PE, Hazel MA, Kaplinski MA, Stevens LE, Hoffnagle TL. 2001. The 1996 controlled flood in Grand Canyon: flow, sediment transport, and geomorphic change. *Ecological Applications* **113**: 657–671 https://doi.org/1890/1051-0761(2001)011(0657:TCFIGC)2.0.CO;2

Schmidt JC, Rubin DM. 1995. Regulated streamflow, fine-grained deposits, and effective discharge in canyons with abundant debris fans. In *Natural and Anthropogenic Influences in Fluvial Geomorphology*, Costa JE, Miller AJ, Potter KW, Wilcock PR (eds). American Geophysical Union: Washington, DC; 45–56.

Smith MW, Carrivick JL, Quincey DJ. 2015. Structure from motion photogrammetry in physical geography. *Progress in Physical Geography* **40**: 247–275 https://doi.org/1177/0309133315615805

Tarboton DG, Bras RL, Rodriguez-Iturbe I. 1991. On the extraction of channel networks from digital elevation data. *Hydrological Processes* **5**(1): 81–100.

Topping DJ, Rubin DM, Vierra LE. 2000. Colorado River sediment transport 1. Natural sediment supply limitation and the influence of Glen Canyon Dam. *Water Resources Research* **36**: 515–542 https://doi.org/1029/1999WR900285

Trimble SW. 1983. A sediment budget for Coon Creek basin in the Driftless Area, Wisconsin, 1853–1977. *American Journal of Science* **283**: 454–474 https://doi.org/2475/ajs.283.5.454

U.S. Bureau of Reclamation. 1998. *Earth Manual, Part 1*, 3rd Edition, Denver, Colorado.

Westoby MJ, Brasington J, Glasser NF, Hambrey MJ, Reynolds JM. 2012. "Structure-from-Motion" photogrammetry: a low-cost, effective tool for geoscience applications. *Geomorphology* **179**: 300–314 https://doi.org/1016/j.geomorph.2012.08.021

Wheaton JM, Brasington J, Darby SE, Kasprak A, Sear D, Vericat D. 2013. Morphodynamic signatures of braiding mechanisms as expressed through change in sediment storage in a gravel-bed river. *Journal of Geophysical Research: Earth Surface* **118**: 759–779 https://doi.org/1002/jgrf.20060

Wheaton JM, Brasington J, Darby S, Merz J, Pasternack GB, Sear D, Vericat D. 2010a. Linking geomorphic changes to salmonid habitat at a scale relevant to fish. *River Research and Applications* **26**: 469–486 https://doi.org/1002/rra.1305

Wheaton JM, Brasington J, Sear D, Darby S. 2010b. Accounting for uncertainty in DEMs from repeat topographic surveys: improved sediment budgets. *Earth Surface Processes and Landforms* **35**: 136–156 https://doi.org/1002/esp.1886

Supporting Information

Additional Supporting Information may be found online in the supporting information tab for this article.